scientific reports

Check for updates

OPEN

Unraveling the luminescence secrets of turquoise nucleus cultivated pearls

Yan Li[1,2,3]✉, Qing Su[2], Wei Shao[1] & Lei Li[2,4]

Turquoise nucleus cultivated (TNC) pearls represent a distinctive variety which are distinguished by their unique nucleus and remarkable aesthetic appeal. In contradistinction to the common pearls, which were formed by a shell nucleus, TNC pearls are characterized by a nucleus composed of a turquoise-like mineral. This study presents a comprehensive analysis of the spectral characteristics of TNC pearls. It reveals that TNC pearls grew in seawater, as indicated by the peak area ratio of Sr to Ca in X-ray fluorescence data. Additionally, the relatively subdued luster of TNC pearls is hypothesized to result from the specific nature of their nucleus material. It is noteworthy that the nuclei of these pearls are not composed of natural turquoise because their infrared spectrum exhibits characteristic absorption peaks of gibbsite at 1025 cm^{-1} and 669 cm^{-1}, alongside peaks indicative of organic compounds. It is proposed that the nucleus consists of a gibbsite, encased within a protective layer of organic compounds during the carving process. In addition, three-dimensional (3D) fluorescence and photoluminescence spectroscopy demonstrate that the fluorescence characteristics of TNC pearls are comparable to those of traditional cultivated pearls. This study analyzes the samples derived from black-lipped oysters and golden-lipped oysters respectively. This finding underscores the efficacy of 3D fluorescence and photoluminescence spectroscopy as reliable methods for identifying these new pearl species.

Keywords Turquoise nucleus cultivated pearls, Spectrum analysis, Fluorescence characteristics, Gibbsite, Black-lipped oyster, Golden-lipped oyster

Historically, pearls have been esteemed for their rich hues and distinctive luster, formed through intricate biological processes primarily composed of aragonite and a minor proportion of organic matter[1]. However, the availability of natural pearls is exceedingly limited compared to the majority of cultivated pearls on the market today[2]. Those various types of pearls include Tahitian pearls, South Sea golden pearls, Akoya pearls from Japan, and Edison pearls cultivated in China.

In recent years, innovative techniques for pearl cultivation have emerged, particularly involving the incorporation of turquoise as a nucleus within the mother oyster, which is then submerged in water for a cultivation period of one to two years. The renowned jewelry company Galatea has adeptly harnessed this technology to produce colored core pearls, intricately carving the layers of the pearls into exquisite jewelry pieces for commercial sale. A schematic diagram (Fig. S1) has been created to enhance the understanding of the growth process of turquoise nucleus cultivated (TNC) pearls, referencing existing research and the sample we have as an illustrative example. The specific growth process description and schematic diagram can be found in the supplementary information.

Current research[3–5] on pearls predominantly focuses on imitations and optimized processed products within the market, with limited in-depth studies addressing new varieties. Previous investigations[6] into TNC pearls have primarily emphasized their aesthetic properties and commercial value. However, there is a notable deficiency in the comprehensive analysis regarding the specific composition of their nuclei and the mother oysters that are responsible for their formation.

This study aims to address this gap by identifying the primary components of the nucleus and the pearl oysters that produce this unique type of pearl. Visually, the nuclei of TNC pearls closely resembles turquoise, but its actual chemical composition still requires further investigation. Turquoise is a hydrous copper aluminum phosphate mineral renowned for its distinctive coloration and luster[7]. However, the majority of natural

[1]Institute for Advanced Marine Research, China University of Geosciences, Guangzhou 511462, China. [2]Gemological Institute, China University of Geosciences, Wuhan 430074, China. [3]Department of Aeronautics, Imperial College London, London SW7 2AZ, UK. [4]Guizhou Geological and Mineral Resources Development Co., Ltd, Guiyang, China. ✉email: yanli@cug.edu.cn

turquoises exhibit relatively low density and high porosity, which often result in surface defects such as light coloration and diminished luster[8]. Consequently, blue turquoise which has compact texture and strong luster commands a premium price in the market. This has led to a large number of treated and imitated products, and the phenomenon of passing off inferior products as good is very common. Currently, common filling agents such as resin and silicate are employed to enhance the structural integrity of turquoise[9]. Additionally, various physical and chemical treatments, including wax impregnation, dyeing, electrochemical treatment, and other methods, are frequently utilized to reduce porosity and improve surface luster and coloration[10]. Furthermore, several less expensive minerals, such as carbonate minerals, variscite, gibbsite, and barite, are often used as imitations for natural turquoise[11,12]. Due to the difficulty to distinguish natural turquoise from these imitations through visual inspection alone, the complexity of the turquoise market has become even greater. Fourier transform infrared (FTIR) spectroscopy is recognized as an effective method for rapidly identifying unknown mineral components, particularly in differentiating natural turquoise from its treated products and imitations[8,13]. And energy-dispersive X-ray fluorescence (EDXRF) permits to reveal the elemental composition of materials[14,15]. In recent years, 3D fluorescence spectroscopy and photoluminescence spectroscopy have gained significant popularity for the identification of various types of pearls and their imitations. Notably, Li et al.[16] proposed that 3D fluorescence spectroscopy can rapidly and intuitively differentiate between natural silver-gray Akoya pearls and irradiated modified pearls. Additionally, Chen et al.[17] summarized the photoluminescence spectral characteristics of various pearl colors, providing a valuable reference for distinguishing between imitations and color-treated pearls.

Given that the same cultivation process was used for all TNC pearls, this study selected two representative TNC pearls for further analysis. In this study, FTIR spectroscopy was employed to analyze the mineral composition of the TNC pearl nucleus and compare it to that of natural turquoise. Furthermore, the spectral characteristics of the pearl layer were examined using EDXRF, 3D fluorescence spectroscopy, and photoluminescence spectroscopy to determine the mother oyster of the TNC pearl samples. The findings support the efficacy of 3D fluorescence and photoluminescence spectroscopies as methods for exploring new varieties of pearl.

Results

Gemological properties of turquoise nucleus cultivated pearls and reference samples

This study selected two TNC pearl samples (I1 and I2), four additional pearls (A1, E1, T1, and G1), as well as one natural turquoise sample (N1) to serve as references (Fig. 1). TNC pearls and other common pearls exhibit a characteristic pearly luster when observed visually. However, it is noteworthy that the luster of samples I1 and I2 is comparatively diminished. The pearl layer of sample I1 presents a grayish-black hue, while sample I2 displays a light gold coloration. The turquoise in both samples exhibits a uniform light blue color without any visible veins and possesses a waxy luster. Upon examination under a gemstone microscope, dispersed dark blue, yellow-green, and brown mineral inclusions are visible within the turquoise (Fig. 2a,b). Additionally, a brown gel-like substance was observed at the interface between the turquoise and the pearl layer (Fig. 2c,d).

A comparative analysis of the surface structures of pearl layers from samples I1 and I2 with those from E1, A1, T1, and G1 reveals that the imbricated structures in I1 and I2 are less pronounced (Fig. 3a,b). In contrast, the

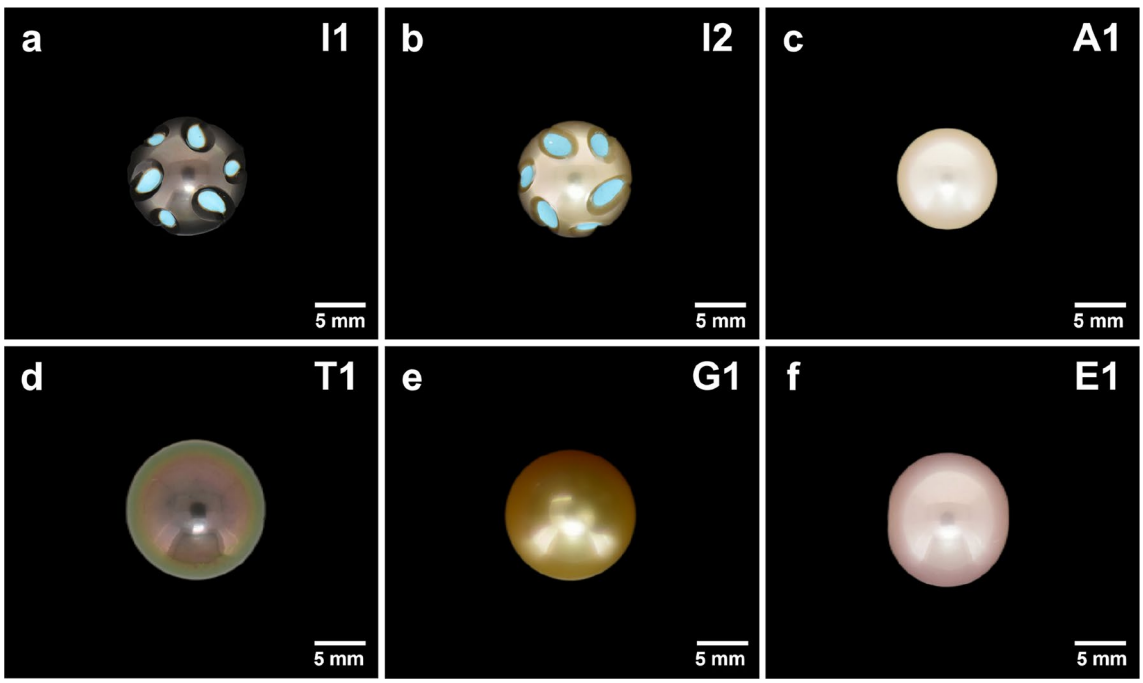

Fig. 1. (**a**, **b**) Two TNC pearl samples I1 and I2, (**c**) one each of Akoya pearl (A1), (**d**) Tahitian pearl (T1), (**e**) golden pearl from south sea (G1), (**f**) Edison pearl (E1).

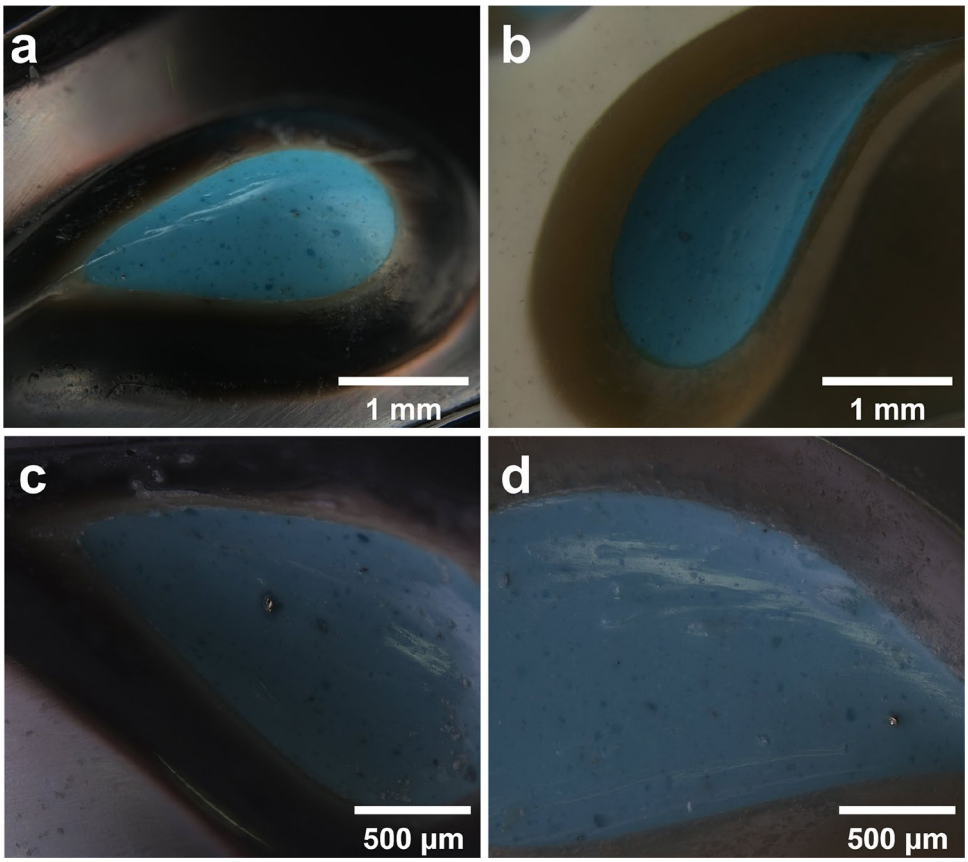

Fig. 2. (**a**, **b**) Details of the turquoise section of two TNC pearl samples I1 and I2, (**c**, **d**) Details of the junction between the pearl layer and the pearl nuclei of TNC pearl I1 and I2.

contour lines on the surfaces of the other common pearls (T1, G1, A1, E1) are denser and more distinctly defined (Fig. 3c–f). This difference in nucleus morphology between I1, I2, and traditional pearl nuclei may contribute to the observed weaker luster.

Under long-wavelength ultraviolet light, only the A1 pearls exhibit strong blue-white fluorescence, while the fluorescence intensity of the pearl layers in samples E1, G1, T1, I1, and I2 is significantly subdued (Fig. 4). The nuclei of samples I1 and I2 display inert fluorescence; however, pronounced white fluorescence is noted at the interface between the pearl layer and the nucleus. This observation, in conjunction with the aforementioned brown gel-like substance, suggests the possible presence of an organic compound. Further analyses are required to ascertain its specific composition.

FTIR spectra of the nuclear components of turquoise nuclear cultivated pearls

The FTIR spectra of the turquoise components found in samples I1 and I2 (IT1 and IT2), as illustrated in Fig. 5a, exhibit marked differences when compared to natural turquoise (sample NT1). The infrared absorption peaks for natural turquoise (Fig. 5b) are located at 3506, 3466, 3278, 3068, 1652, 1130, 1012, and 836 cm^{-1}. Specifically, the peaks at approximately 3506 cm^{-1} and 3466 cm^{-1} are associated with the stretching vibrations of structural hydroxyl groups (OH^-), while the peak at 836 cm^{-1} corresponds to the bending vibrations of OH^-. Additionally, the peaks at 3278 cm^{-1} and 3068 cm^{-1} are attributed to the stretching vibrations of crystal water (H_2O), while the peak at 1652 cm^{-1} corresponds to the bending vibrations of crystal water. The peaks at 1130 cm^{-1} and 1012 cm^{-1} represent the stretching vibrations of phosphate ions (PO_4^{3-})[8,18,19]. And the infrared spectra of samples I1 and I2 were also compared with those of filled turquoise (FT1) and compressed carbonate powder imitation turquoise (CIT1) (Fig. 5b). It is evident that the filled turquoise exhibits a spectral profile remarkably similar to that of natural turquoise; however, characteristic absorption bands of the filling material are observed, notably the CH_2 stretching vibrations at 2926 cm^{-1} and 2855 cm^{-1}, as well as the C=O stretching vibration at 1727 cm^{-1}[10]. Conversely, the infrared spectra of carbonate imitation turquoise display distinct features, with antisymmetric stretching vibrations of carbonate groups appearing at 1513 cm^{-1} and in-plane bending vibrations observed at approximately 890 and 746 cm^{-1}[20]. Additionally, the absorption peak associated with artificial resin is present, located around 2926 and 2852 cm^{-1}. Obviously, whether it is filling treated turquoise or pressing carbonate powder imitation turquoise, the infrared spectra are significantly different from those of I1 and I2.

Conversely, the infrared spectrum of TNC pearl samples exhibits significant similarity to the reference spectrum (G1) of gibbsite. Characteristic absorption bands were identified at the following wavenumbers: 3618, 3525, 3446, 3374, 2925, 2869, 1730, 1276, 1143, 1025, 800, 748, and 669 cm^{-1}. The peaks at 3618 cm^{-1},

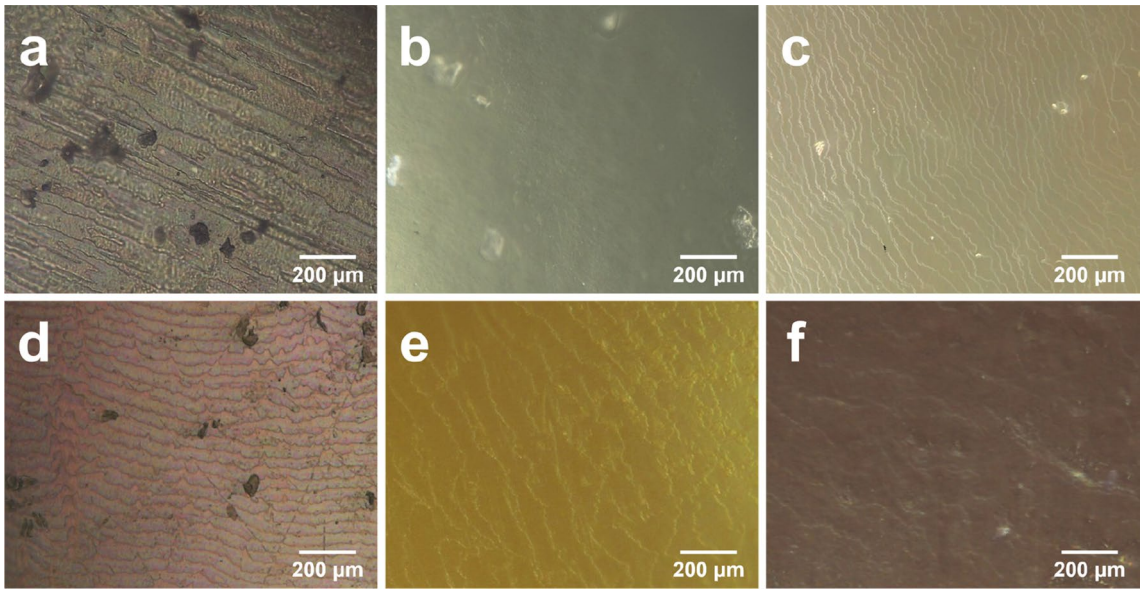

Fig. 3. The surface features of (**a**, **b**) two TNC pearl samples I1 and I2, (**c**–**f**) reference samples A1, T1, G1, E1.

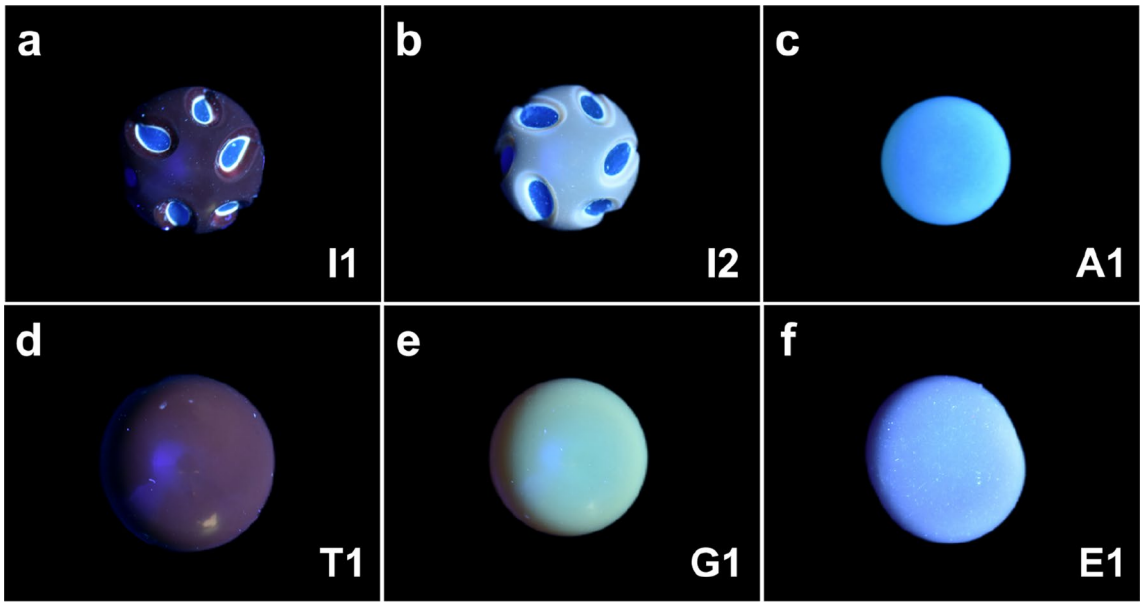

Fig. 4. Fluorescence of (**a**–**b**) two TNC pearl samples I1 and I2, (**c**–**f**) reference samples A1, T1, G1, E1 under long wavelength ultraviolet light.

3525 cm^{-1}, 3446 cm^{-1}, and 3374 cm^{-1} are assigned to -OH stretching vibrations. Peaks observed at approximately 800 cm^{-1} and 748 cm^{-1} correspond to -OH bending vibrations. The peak at 1025 cm^{-1} is attributed to the Al-O–H stretching vibration, while the band near 669 cm^{-1} is indicative of Al-O–H bending vibration[21]. These absorption features collectively constitute the diagnostic spectral signature of gibbsite, confirming that samples IT1 and IT2 are predominantly composed of this mineral.

Furthermore, the spectra of IT1 and IT2 reveal the presence of organic components absent in pure gibbsite. This suggests that IT1 and IT2 likely contain organic compounds, potentially resulting from the pressing of gibbsite powder with an organic binder. Distinctive evidence for organic constituents includes pronounced aliphatic C-H stretching vibrations at 2925 cm^{-1} and 2869 cm^{-1}. A well-defined carbonyl (C = O) stretching vibration is observed at 1730 cm^{-1}, while a peak associated with C–O–C stretching appears at 1143 cm^{-1}. The absorption peak at 1276 cm^{-1} arises from -OH deformation, and the band at 968 cm^{-1} signifies the bending vibration of unsaturated hydrocarbon groups (= C-H). Based on these spectral characteristics, the organic component is inferred to be a resinous compound[21,22]. The abnormal intensity of these organic absorption peaks

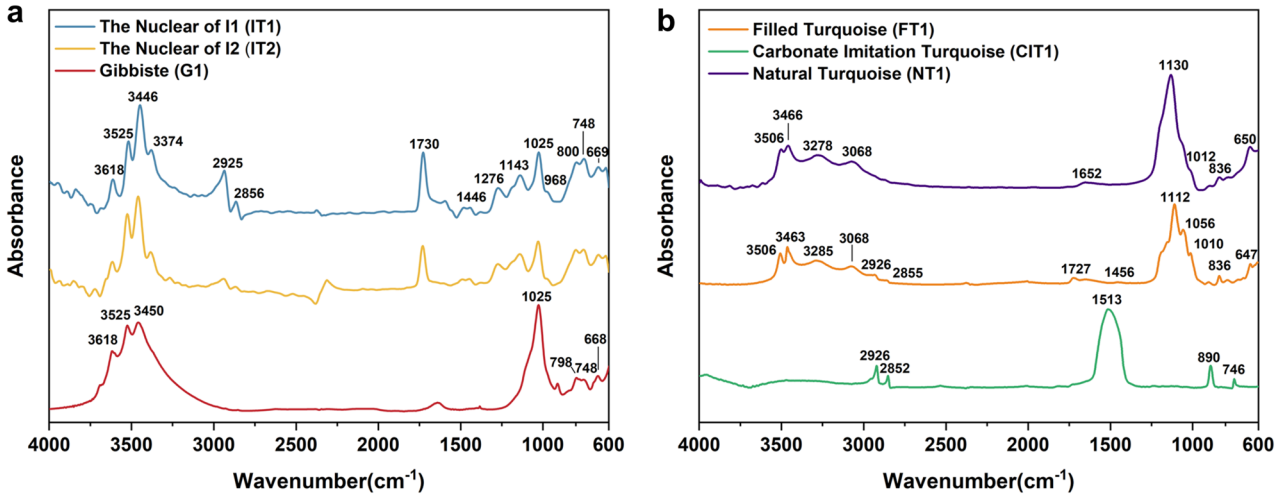

Fig. 5. (**a**) FTIR spectra of the nuclei of TNC pearl samples (IT1, IT2), and gibbsite (G1), (**b**) FTIR spectra of natural turquoise (NT1), filled turquoise (FT1) and compressed carbonate powder imitation turquoise (CIT1). Spectra are offset vertically for clarity.

suggests that their origin cannot be solely attributed to fillers within the nuclear. It is plausible that they are associated with the gelatinous material previously observed at the interface between the layer and the nuclear.

In summary, the analytical evidence of the FTIR spectra in Fig. 5 indicates that the nuclei in samples I1 and I2 are not natural turquoise, but rather a synthetic imitation primarily composed of gibbsite, potentially incorporating minor organic constituents. In addition, gel-like substances observed at the interface of the pearl layer and nuclear may play a role in enhancing pearl quality. It is hypothesized that these substances could be pre-treatment coatings applied to the imitation turquoise nuclei before inserting nuclear, aiming to improve biocompatibility between the nuclear and the oyster, and to prevent rejection reactions that could lead to expulsion of the nuclear. Alternatively, they may serve to fill pits and micro-damages on the surface of the pearl nuclear caused by carving, thereby improving both the appearance and structural integrity of the pearl. However, the exact distribution of these organic compounds and their functions in improving pearl quality remain largely speculative and have not been fully characterized. Limitations in current non-destructive testing methods hinder further exploration of this interface, highlighting a key avenue for future research.

EDXRF analysis of turquoise nucleus cultivated pearls and reference samples

EDXRF testing was conducted on the samples described in this study to elucidate the growth environment—specifically, whether seawater or freshwater—of samples I1 and I2. Previous research[23,24] has established that the strontium (Sr) content in pearls from seawater is significantly higher than that present in pearls from freshwater sources. Notably, sample E1 is confirmed to be a freshwater pearl, while samples A1, T1, and G1 have been identified as seawater pearls. It can be seen that the E1 sample exhibits a diminished Sr peak relative to the other five samples through observing the intensity of the Sr peak in the EDXRF spectrum, suggesting that samples I1 and I2 are likely seawater pearls, although further verification is warranted. The specific EDXRF spectrum of pearl samples is available in supplementary information (Fig. S2).

Previous research[25] indicates that integrating the Kα peaks of Sr and Ca in the spectrum to determine their respective areas and comparing these values, the Sr/Ca counting ratio can be obtained for assessing the growth environment of pearls. Typically, the Sr/Ca ratio of seawater pearls exceeds 0.3, whereas that of freshwater pearls is generally below this threshold. In the present study, the Sr/Ca ratio was computed by analyzing the integrated areas of the calcium and strontium elemental peaks. The resulting Sr/Ca values for samples I1, I2, A1, G1, and T1 all exceed 0.3, suggesting a seawater growth environment, while the Sr/Ca ratio for sample E1 remains below 0.3 (Table 1). Therefore, it can be inferred that the pearl layers of samples I1 and I2 likely originated in a seawater environment. Nonetheless, additional testing is essential to further investigate the specific mother oysters responsible for the formation of the pearls in samples I1 and I2.

Fluorescence characteristics of turquoise nucleus cultivated pearls and reference samples

A series of 3D fluorescence tests were conducted on the pearl layers of six samples to elucidate further the identity of the mother oysters responsible for the production of the pearl layers in samples I1 and I2 (Fig. 6). The results indicate that the fluorescence intensities of I1 and I2 are relatively low with a prominent luminescent center that exhibits the highest fluorescence intensity at excitation/emission (E_x/E_m) wavelengths of approximately 284/334 nm.

Comparative analysis of the 3D fluorescence spectra of I1 and I2, alongside other samples, aids in classifying their respective pearl types. The fluorescence intensities of samples E1 and A1 are several times greater than those of I1 and I2 (Fig. 6e-f). Notably, A1 exhibits two distinct fluorescence emission centers at 446 nm and 464 nm when excited at a wavelength of 374 nm, a pattern that is markedly different from those observed in I1

Samples	Integral area of Sr/Ca
E1	0.174
T1	0.549
A1	0.411
G1	0.547
I1	0.371
I2	0.556

Table 1. The Sr/Ca ratio of TNC pearl samples I1, I2 and reference samples G1, T1, A1, E1.

and I2 (Fig. 6a, b). Furthermore, it has been confirmed that I1 and I2 are not freshwater pearls, while E1 displays a significantly strong fluorescence intensity. Consequently, it can be confidently concluded that I1 and I2 do not belong to the categories of Edison pearls or Akoya pearls.

The fluorescence center of T1 is located at approximately E_x/E_m 284/336 nm (Fig. 6c), closely resembling that of I1. Both samples exhibited low fluorescence intensities, remaining below 100. Additionally, I1 and T1 display fluorescence peaks at E_x/E_m wavelengths of 232/336 nm and 222/274 nm, respectively. This indicates that I1 can be classified as a Tahitian pearl.

The 3D fluorescence spectrum of I2 shows similarities to those of I1 and T1; however, its fluorescence intensity is notably stronger, approaching 200, and is more comparable to that of G1 (Fig. 6d). The strongest fluorescence centers for both I2 and G1 are similarly positioned to those of T1 and I1. Nevertheless, the peak shape at the 335 nm emission (E_m) differs from that of I1 and T1, as it exhibits a shoulder peak. Additionally, there is no fluorescence peak at the E_x/E_m wavelength of approximately 222/274 nm. Therefore, it can be concluded that I2 does not fit into the category of Tahitian pearls, but rather belongs to the category of golden pearls from the South Sea.

Photoluminescence spectroscopy analysis of turquoise nucleus cultivated pearls and reference samples

The photoluminescence spectra of the samples analyzed in this study were examined, revealing distinct fluorescence backgrounds among the different types of pearls (Fig. 7). To accurately differentiate between the pearl types I1 and I2, the ratio of the overall fluorescence intensity (F) to the main peak intensity of aragonite at 564 nm (A) was calculated to assess the intensity of their fluorescence background (Table 2)[17].

The spectral peak shapes of I1 and I2 exhibit notable similarities; however, their fluorescence background intensities differ significantly, indicating that they do not represent the same type of pearl (Fig. 7). Further analysis indicates that I1 resembles T1, as demonstrated by a notably weak intensity of the aragonite peak at 564 nm, accompanied by an exceptionally strong fluorescence background. The F/A value for I1 reaches up to 45, with emission peaks observed at 620 nm and 650 nm. In contrast, the F/A value for I2 is relatively similar to those of A1 and G1. However, previous 3D fluorescence spectra have demonstrated that the fluorescence center of A1 is entirely distinct from that of I2, further confirming that I2 and G1 originate from the same type of oyster: the cultivated golden-lipped oyster. Additionally, the F/A values for the photoluminescence spectra of I1 and I2 are higher than those of the ordinary pearls T1 and G1, suggesting that the incorporation of turquoise as the nucleus enhances their fluorescence background.

Discussion

In comparison to common pearls, TNC pearls exhibit a less distinct imbricated structure and possess inferior luster. This disparity is likely due to their unconventional nucleus, which leads to a less dense layer of pearl. Infrared spectroscopy analysis has shown that their nuclei are made of gibbsite rather than natural turquoise. Moreover, gel-like substances observed at the pearl-nucleus interface may enhance pearl quality, potentially serving as pre-treatment coatings on imitation turquoise nuclei to improve biocompatibility or as fillers for carving-resulted pits and micro-damages to refine appearance and integrity, but this speculation has limitations and requires further research. The spectral characteristics of samples I1 and I2 resemble those of common pearls. This study utilized a combination of techniques, including energy dispersive EDXRF, 3D fluorescence spectroscopy, and Photoluminescence spectroscopy, to differentiate the mother oysters of these pearls. Notably, the growth environment of TNC pearls could be identified through the peak area ratio of Sr to Ca in EDXRF, and 3D fluorescence testing emerged as the most rapid and effective method, facilitating intuitive categorization of the pearls. The spectral data indicate that the mother oysters of the two TNC pearls are from black-lipped oysters (*Pinctada margaritifera*), which produce Tahitian pearls, and gold-lipped oysters (*Pinctada maxima*), known for producing golden pearls. This comprehensive analysis of TNC pearls enhances the understanding of this emerging category and contributes significantly to the broader field of pearl research. The emergence of TNC pearls has led to the development of new types of cultured pearls which were cultured through other kinds of colored gems like imitation turquoise, opal, and coral as nucleus, expanding the possibilities for pearl jewelry design and leading to an increase of the pearl prices in the jewelry market.

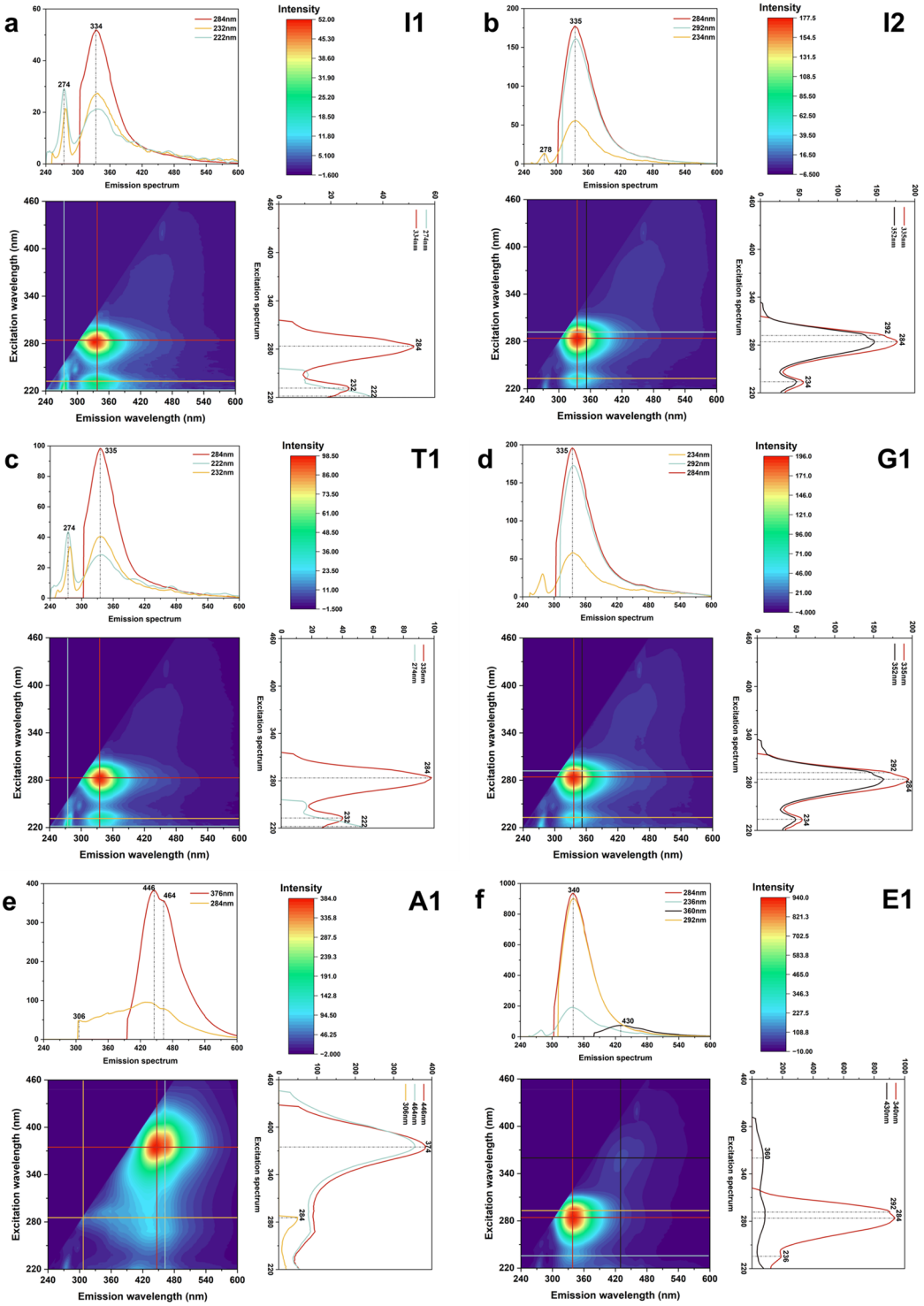

Fig. 6. 3D fluorescence spectra of (**a**–**b**) TNC pearl samples I1 and I2, (**c**–**f**) reference samples G1, T1, A1, E1.

Methods

FTIR spectroscopy

A Bruker Vertex 80 FTIR spectrometer was used to analyze the primary components of the pearl nucleus. Using attenuated total reflectance infrared spectroscopy, place the test positions of samples (I1, I2, N1, R1, R2, R3) at the infrared light source for testing. The FTIR spectra were acquired over a range of 400–4000 cm^{-1} with a resolution of 4 cm^{-1}, accomplished by accumulating a total of 64 scans. Perform Kramers–Kronig transformation on the collected reflectance spectra to convert them into infrared absorption spectra.

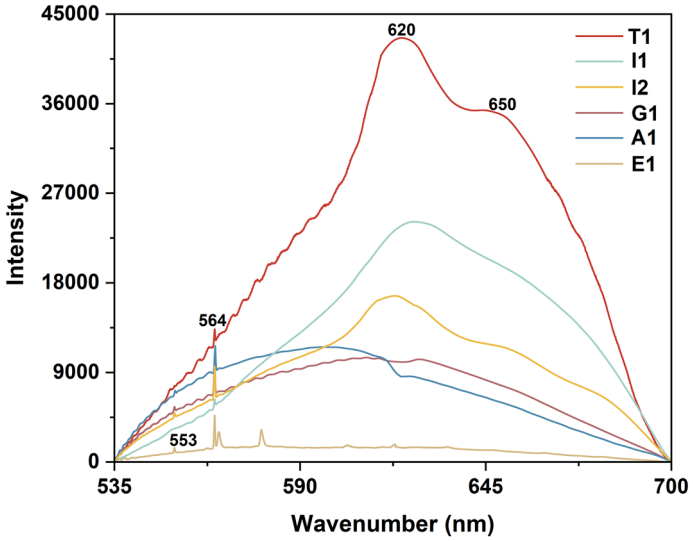

Fig. 7. Photoluminescence spectrum of TNC pearl samples I1, I2 and reference samples G1, T1, A1, E1. Spectra are offset vertically for clarity.

Samples	F/A
I1	45.00
I2	5.42
T1	37.23
G1	3.25
A1	4.70
E1	0.52

Table 2. The F/A of TNC pearl samples I1, I2 and reference samples G1, T1, A1, E1.

EDXRF spectroscopy

EDXRF spectroscopy was conducted using a Thermo ARL Quant'x EDXRF Analyzer under specific test conditions for the pearl layers of intact pearls. Palladium (Pd) was utilized as the target material and operated at a maximum voltage of 28 kV under vacuum conditions. Each test lasted for 60 s to ensure the accuracy of the results.

3D fluorescence spectroscopy

The 3D fluorescence spectroscopy measurements of intact pearl samples were performed using a Jasco FP-8500 spectrofluorometer equipped with a xenon lamp. The parameters for this measurement included an excitation bandwidth of 5 nm and an emission bandwidth of 2.5 nm. The excitation range was set between 220 and 500 nm in 2 nm intervals, while the emission range was set from 240 to 600 nm in 1 nm intervals. The tests were conducted under a voltage of 300 V with a scanning velocity of 1,000 nm/min.

Photoluminescence spectroscopy

Samples of intact pearls (I1-2, A1, T1, E1, G1) were analyzed using a JASCO NRS7500 Raman spectrometer. The spectra were obtained with a 532 nm laser, delivering approximately 4.7 mW of power onto the sample. An MPLFLN 20 × objective lens and an L600/B500 nm diffraction grating were employed. Data collection occurred over the wavelength range of 535 to 700 nm, with each spectrum integrated for 5 s and the measurement repeated twice.

Data availability

Data will be made available on request. If someone wants to request the data from this study, please contact professor Yan Li at yanli@cug.edu.cn.

Received: 28 March 2025; Accepted: 21 July 2025
Published online: 06 August 2025

References

1. Micieli, D. et al. Characterizing pearls structures using X-ray phase-contrast and neutron imaging: A pilot study. *Sci. Rep.* **8**, 12118 (2018).
2. Edeline, P.-E., Leclercq, M., Le Luyer, J., Chabrier, S. & Droit, A. Pearl shape classification using deep convolutional neural networks from Tahitian pearl rotation in Pinctada margaritifera. *Sci. Rep.* **13**, 13122 (2023).
3. Lee, J. H. *et al.* Birefringence analysis of cultured and imitation pearls using polarization-sensitive swept-source OCT. In *Optical Methods in Developmental Biology* **8593** (2013).
4. Zhou, C. H. et al. Identification of "Pistachio" colored pearls treated by Ballerina Pearl Co. *Gems Gemol.* **52**, 50–59 (2016).
5. Zhou, C. H. et al. Detection of Color treatment and optical brightening in Chinese freshwater "Edison" pearls. *Gems Gemol.* **57**, 124–134 (2021).
6. Hsu, T., Homkrajae, A. & Schumacher, K. Never stop innovating: Gem artist Chi Huynh. *Gems Gemol.* **58**, 458–473 (2022).
7. Huang, L. Y. et al. Composition and spectral characteristics of porcelain-treated turquoise. *Gems Gemol.* **58**, 438–457 (2022).
8. Schwarzinger, B. & Schwarzinger, C. Investigation of turquoise imitations and treatment with analytical pyrolysis and infrared spectroscopy. *J. Anal. Appl. Pyrol.* **125**, 24–31 (2017).
9. Han, W., Lu, T. J., Dai, H. R., Su, J. & Dai, H. Impregnated and dyed turquoise. *Gems Gemol.* **51**, 343–345 (2015).
10. Liu, L. et al. Technical evolution and identification of resin-filled turquoise. *Gems Gemol.* **57**, 22–35 (2021).
11. Yang, C. Y., Wang, T. T., Zhang, W. X. & Tang, W. X. Study on spectral characteristics of turquoise imitations of single and multiple component mixtures. *Spectrosc. Spectr. Anal.* **45**, 183–190 (2025).
12. Yan, J. et al. Determination of mineral compositions of new imitated turquoise by FTIR-XRD-XRF. *Rock Min. Anal.* **34**, 544–549 (2015).
13. Taniguchi, Y., Hirao, Y., Shimadzu, Y. & Tsuneki, A. The first fake? Imitation turquoise beads recovered from a Syrian Neolithic site, Tell El-Kerkh. *Stud. Conserv.* **47**, 175–183 (2002).
14. Hatipoğlu, M. & Başevirgen, Y. Photoluminescence of Turkish purple jade (turkiyenite). *J. Lumin.* **132**, 2897–2907 (2012).
15. Filosa, R. et al. Nonlinear optical effects in natural topaz. *J. Lumin.* **263**, 120076 (2023).
16. Li, Y. J., Chen, C. Y. F. & Li, L. P. Spectroscopy study of γ-ray irradiated Gray Akoya pearls. *Spectrosc. Spectr. Anal.* **43**, 1056–1062 (2023).
17. Chen, C. Y. F. & Li, L. P. The application of photoluminescence spectra on identification of different types of pearls. *Spectrosc. Spectr. Anal.* **42**, 20–25 (2022).
18. Zhao, A. D. et al. Study on spectroscopic characteristics of turquoise treated with phosphate and porcelain. *Spectrosc. Spectr. Anal.* **43**, 1192–1198 (2023).
19. Djelloul, A., Aida, M. S. & Bougdira, J. Photoluminescence, FTIR and X-ray diffraction studies on undoped and Al-doped ZnO thin films grown on polycrystalline α-alumina substrates by ultrasonic spray pyrolysis. *J. Lumin.* **130**, 2113–2117 (2010).
20. Yang, C. Y., Wang, T. T., Zhang, W. X. & Tang, W. X. Study on spectral characteristics of turquoise imitations of single and multiple component mixtures. *Stud. Conserv.* **45**, 183–190 (2025).
21. Xu, H. Y. & Yu, X. Y. Pressed gibbsite and calcite as a rhodochrosite imitation. *Gems Gemol.* **55**, 406–415 (2019).
22. Xu, F. S., Chen, Q. L., Ding, W. & Wang, H. T. Study on fluorescence spectrometry of natural and organic filling treated turquoise. *Spectrosc. Spectr. Anal.* **41**, 2918–2923 (2021).
23. Zhang, E., Huang, F. Q., Wang, Z. T. & Li, Q. Characteristics of trace elements in freshwater and seawater cultured pearls. *Spectrosc. Spectr. Anal.* **34**, 2544–2547 (2014).
24. Sakakura, I., Tsuchida, H., Sasaki, Y. & Hayashii, H. Elemental analysis of cultured pearls by PIXE. *Int. J. PIXE* **27**, 93–99 (2017).
25. Zhu, H. W. et al. Application of energy dispersive X-ray fluorescence spectroscopy in gemology. *China Insp. Body Lab.* **32**, 56–61 (2024).

Acknowledgements

This work was supported by Annual Key Project of Modern Public Visual Art Design Research Center—Research on the Protection, Inheritance and Innovation of Ancient Chinese Accessory Culture in the Digital Age (No.JD-2024-03), "CUG scholar" Scientific Research Funds at China University of Geosciences, Wuhan (No. CUG2022185), Guangzhou Youth Top Talent Program, China Arts and Crafts Society 2024 Arts and Crafts Research Project, Case Study on the Development and Brand Building of Tianjin Silk Craft Industry (No. CNACS2024-I-3). Many thanks to Mr. Masaki Furuya from Japan Germany Gemmological Laboratory for providing us the CHNC pearls.

Author contributions

Y.L.: Date curation, investigation, analyzed and discussed the results. Q.S.: Investigation, wrote original draft, analyzed and discussed the results. W.S. and L.L.: Supervised the experiments. All authors have reviewed the manuscript.

Declarations

Competing interests

The authors declare no competing interests.

Additional information

Supplementary Information The online version contains supplementary material available at https://doi.org/10.1038/s41598-025-12814-w.

Correspondence and requests for materials should be addressed to Y.L.